Science World Journal Vol. 20(No 3) 2025 https://dx.doi.org/10.4314/swj.v20i3.21
www.scienceworldjournal.org
ISSN: 1597-6343 (Online), ISSN: 2756-391X (Print)
Published by Faculty of Science, Kaduna State University

SOLVENT-DEPENDENT SYNTHESIS AND OPTICAL CHARACTERIZATION OF IRON OXIDE (Fe_2O_3) NANOPARTICLES VIA COPRECIPITATION METHOD

*[1]Alhassan Aliyu, [1]Jibrin Alhaji Yabagi, [1]Mohammad Bello Ladan & [1,2]Firdausi Adamu Erena

[1]Department of Physics, Faculty of Natural Sciences, Ibrahim Badamasi Babangida University, Lapai, Niger State
[2]Department of Physics, School of Science, Federal University of Education, Kontagora

*Corresponding Author Email Address: aliymen001@gmail.com, jibrinyabagi@ibbu.edu.ng

ABSTRACT
Nanostructured metal oxides, particularly iron oxide (Fe_2O_3), have attracted considerable interest because of their unique optical and magnetic properties and due to their wide applications in catalysis, sensors, magnetic devices, and environmental remediation. This study investigates the solvent-dependent synthesis of iron oxide (Fe_2O_3) nanoparticles via a co-precipitation method using distilled water, ethanol, and a water–ethanol (1:1) mixture, with a focus on tailoring structural and optical properties for advanced applications. Iron chloride precursors were co-precipitated under alkaline conditions (pH 10), followed by filtering and drying at 80 °C to yield crystalline Fe_2O_3. Fourier-transform infrared (FTIR) spectroscopy confirmed Fe–O vibrational modes (550–700 cm^{-1}) and solvent-specific surface chemistry: water-synthesized nanoparticles exhibited strong O–H stretching (3400 cm^{-1}) and bending (1630 cm^{-1}) modes, indicative of hydroxylation, while ethanol-derived samples showed minimal surface hydration but residual C–H/C–O bands (2800–2900 cm^{-1}). UV-Vis spectroscopy revealed solvent-mediated bandgap tuning, with ethanol producing smaller nanoparticles (≈30 nm) and a reduced bandgap of 2.1 eV due to quantum confinement, compared to water-synthesized particles (≈37 nm, 2.58 eV). The water–ethanol mixture yielded intermediate properties, balancing nucleation kinetics and colloidal stability. These findings underscore the critical role of solvent polarity in modulating crystallinity, particle size, and surface chemistry. Ethanol's low dielectric constant minimized agglomeration and enhanced optical absorption in the visible spectrum, positioning ethanol-derived Fe_2O_3 as a promising candidate for photocatalysis and solar energy harvesting. Conversely, water-synthesized nanoparticles, with hydroxyl-rich surfaces, show potential for biomedical applications. This work advances solvent engineering as a sustainable, tunable strategy for optimizing Fe_2O_3 nanomaterials, offering insights into scalable synthesis routes for targeted technological applications.

Keywords: Iron oxide, Coprecipitation, FTIR, UV-Vis, Ethanol, Nanoparticles, Solvents

INTRODUCTION

Nanostructured metal oxides, particularly iron oxide (Fe_2O_3), nanoparticles (IONPs), commonly known as hematite, have emerged as a cornerstone of nanotechnology due to their unique magnetic, optical, and catalytic properties, coupled with low toxicity and environmental compatibility (Ajinkya et al., 2020; Tabassum et al., 2023). Hematite (Fe_2O_3) nanoparticles exhibit tunable magnetic, optical, and chemical properties that have garnered significant attention for applications in catalysis, energy conversion, environmental remediation, and biomedicine (Pourmadadi et al., 2022). The polymorphic nature of iron (III) oxide, combined with its chemical stability and biocompatibility, underlies its versatility in functions ranging from drug delivery vehicles to photocatalysts for pollutant degradation (Ali et al., 2016a; Girardet et al., 2024; Lassoued et al., 2017).

Among various synthetic strategies, including sol–gel, hydrothermal, and thermal decomposition, the chemical coprecipitation method is widely favored for its simplicity, low cost, and scalability in producing (Fe_2O_3) nanoparticles with controlled size and morphology Ibrahim & Abubakar (2013). In this approach, ferric and ferrous salts are co-precipitated under alkaline conditions, yielding iron hydroxides that, upon subsequent thermal treatment, afford crystalline hematite (Soflaee et al., 2015). The rapid nucleation kinetics inherent to coprecipitation facilitate the generation of uniform nanoparticles, while process parameters such as pH, temperature, and ionic strength enable fine-tuning of particle characteristics(Attia et al., 2022; Mansour et al., 2018)

The choice of solvent during coprecipitation exerts a profound influence on nucleation and growth kinetics, particle dispersion, and surface chemistry, with solvents of differing polarity and dielectric properties modulating ion diffusion and aggregation tendencies (Farahmandjou & Soflaee, 2015; Lassoued et al., 2017; Hui & Salimi, 2020). Compared to distilled water, which promotes rapid hydrolysis and larger agglomerates, ethanol's lower polarity and viscosity slow hydrolysis rates, yielding smaller primary particles with increased colloidal stability (Lassoued et al., 2017). A mixed solvent system of water and ethanol can thus offer a balance between nucleation rate and growth control, enabling intermediate particle sizes and tailored surface functionalities (Girardet et al., 2024)

Fourier-transform infrared spectroscopy (FTIR) serves as a fundamental tool to verify hematite formation by detecting characteristic Fe–O vibrational modes in the 400–650 cm^{-1} range and to identify residual hydroxyl or organic impurities arising from solvent interactions (Lassoued et al., 2017). Ultraviolet–visible (UV–Vis) spectroscopy further elucidates the optical properties of Fe_2O_3 nanoparticles, with absorption edges around 450–600 nm corresponding to electronic transitions whose energies can be quantified via Tauc-plot analysis Khalaji & Jafari (2023). Estimation of direct and indirect bandgap energies from UV–Vis data provides insights into the influence of size, crystallinity, and surface states on the electronic behavior of the synthesized nanoparticles (Ali et al., 2016b; Khalaji & Jafari (2023).

Chakraborty et al (2024) note that Iron oxide nanoparticles (Fe_2O_3 NPs) were synthesized using iron chloride hexahydrate ($FeCl_3 \cdot 6H_2O$) and ammonia solution through a straightforward co-

precipitation method. The nanoparticles were annealed at temperatures of 100 °C, 300 °C, 500 °C, 700 °C, and 900 °C, with one sample left unannealed. Comprehensive analyses were performed for structural and optical properties. The XRD patterns confirmed the presence of both Maghemite (γ-Fe_2O_3) and Hematite (α-Fe_2O_3) phases, with a phase transition observed between 100 °C and 300 °C, and the most pronounced transition occurring at 500 °C. At this optimal temperature, the crystallite size was 19.14 nm, the average particle size was 37.36 nm, and the band gap energy was measured at 1.76 eV. These findings suggest that 500 °C is the optimal annealing temperature for producing Fe_2O_3 NPs with desirable properties for applications in targeted drug delivery, MRI contrast enhancement, and environmental remediation. This research advances the engineering of Fe_2O_3 NPs, paving the way for their use in various technological applications.

In this study, α- Fe_2O_3 nanoparticles were synthesized by chemical coprecipitation due to its simplicity, low cost, high yield, and excellent control over the final particle properties through easily adjustable reaction parameters of $FeCl_3 \cdot 6H_2O$ and $FeCl_2 \cdot 4H_2O$ precursors (molar ratio 2:1) in three solvent systems distilled water, absolute ethanol, and a 1:1 (v/v) water–ethanol mixture, under alkaline conditions (pH ≈ 10). After precipitation, the solids were aged, washed with distilled water, Acetone and ethanol, dried at 80 °C, and finally calcined at 400 °C for 3 h to induce phase crystallization. Fourier-transform infrared (FTIR) spectra were recorded (4000–400 cm^{-1}, 4 cm^{-1} resolution) to confirm Fe–O lattice vibrations and detect surface hydroxyls. Ultraviolet–visible (UV–Vis) absorption (200–800 nm) was used to evaluate optical bandgaps via Tauc-plot analysis.

MATERIALS AND METHODS

Materials

Iron III chloride hexahydrate (Ferric chloride) ($FeCl_3 \cdot 6H_2O$, ≥99%), Iron (II) tetraoxosulphate (VI) heptahydrate (Ferrous sulphate) ($FeSO_4 \cdot 7H_2O$), ≥99%), Ammonia solution (NH_4OH, ≥98%), and hydrochloric acid (HCl, 37%) were purchased from Sigma-Aldrich. Absolute ethanol (EtOH, 99.9%) and distilled water were used as received. All glassware was cleaned with acid, rinsed thoroughly with deionized water, and dried before use (Fouad et al., 2019; Kumar et al., 2021).

Synthesis of Fe_2O_3 Nanoparticles

Coprecipitation in Distilled Water

A precursor solution was prepared by dissolving 100 cm^3 of ferric chloride and 50 cm^3 of ferrous sulfate distilled water and was then transferred into a 250 cm^3 beaker acidified to pH 1 with 1 M HCl (Ibrahim & Abubakar, 2013). The solution was heated to 60 °C under nitrogen atmosphere with vigorous stirring at 750 rpm. the solution was precipitated by dropwise addition of ammonia solution at the rate of 1 cm^3 per minute for 1 hour until pH 10 was reached, yielding an orange-brown precipitate. The mixture was stirred for an additional 60 min at 80 °C to complete growth, hour while maintaining the agitation rate (Fouad et al., 2019).

Coprecipitation in Ethanol

An analogous procedure was carried out with 150 cm^3 absolute ethanol as the solvent. Fe salts were dissolved in ethanol at 60 °C, followed by dropwise addition of ammonia solution at the rate of 1 cm^3 per minute for 1 hour until pH 10 was reached, yielding an orange-brown precipitate. Due to ethanol's lower polarity, nucleation was slower and produced finer nuclei (Lassoued et al., 2017).

Coprecipitation in Water–Ethanol Mixture

A 1:1 (v/v) mixture of deionized water and ethanol was used to prepare the precursor solution under the same conditions. This mixed solvent moderated hydrolysis and growth rates, leading to intermediate particle sizes (Girardet et al., 2024).

After precipitation in all three solvent systems, the solids were collected by filtration, washed three times with distilled water and twice with acetone, then dried at 60 °C for 24 hours to obtain Fe_2O_3 (Attia et al., 2022; Mansour et al., 2018).

Characterization Techniques

Fourier-Transform Infrared Spectroscopy (FTIR)

In this study, Fourier transformation infrared spectroscopy (FTIR) analysis was done using a Perkin Elmer FTIR Spectrometer LR 64912C; N3896 coupled with universal Attenuated Total Reflectance (ATR) sample stage and spectrum express FTIR software V1.3.2 Perkin Elmer LX100877-1. With a resolution of 4 cm^{-1}, the sample molecular structure is identified within the 4000–400 cm^{-1} range. ATR-FTIR spectra analysis of the samples was performed to confirm the molecular structure of the materials.

Ultraviolet–Visible Spectroscopy (UV–Vis)

In this study, UV-Vis spectroscopy was used to measure the change in the amount of absorbed UV and visible radiation, the absorption properties of synthesized samples were analyzed by using UV-Vis spectrophotometer (Shimadzu UV-3101PC) at room temperature. A small amount of colloid sample was transferred into a 1 cm path length sampling quartz cuvette for analysis, using deionized water as a reference with a wavelength (λ) range from 300-600 nm Farahmandjou & Soflaee (2015).

RESULTS AND DISCUSSION

Interpretation of FTIR Spectra for Solvent-Dependent Fe_2O_3 Nanoparticles

The FTIR spectra of Fe_2O_3 nanoparticles synthesized via co-precipitation in three solvents; water, ethanol, and a water–ethanol mixture is analyzed below to elucidate solvent-induced structural and surface chemical variations.

FTIR Spectrum of Fe_2O_3 Synthesized in Distilled Water

The chemical structure of the synthesized material was analyzed using Fourier-Transform Infrared (FTIR) spectroscopy. Figure 1 shows the FTIR spectrum recorded in the wavenumber range of 4000 to 400 cm^{-1}. This analysis aims to identify the characteristic vibrational modes of the chemical bonds within the sample, confirming its composition. The FTIR spectrum of water-synthesized Fe_2O_3 (Figure 1) exhibits characteristic broad peak around 3221.3 cm^{-1}, 789.5 cm^{-1} and 680.1 cm^{-1} assigned to the vibrations of O–H stretching vibrations of water molecules physically adsorbed on the surface of the Fe_2O_3 nanoparticles, which suggest that Fe_2O_3 are hydrophilic in nature, Fe–O–Fe bending vibrations of Fe_2O_3 which confirms the structure of Fe_2O_3 and the Fe-O stretching vibrations of hematite signifying the presence of iron oxide phase respectively (Wang et al., 2013). While the peak at 1626 cm^{-1} arises from H–O–H bending modes, indicative of residual moisture Hui & Salimi (2020). The relatively broad Fe–O peaks suggest moderate crystallinity and possible surface hydroxylation, which is typical for aqueous-phase synthesis due to water's high polarity promoting hydroxyl group adsorption

Khalaji & Jafari (2023).

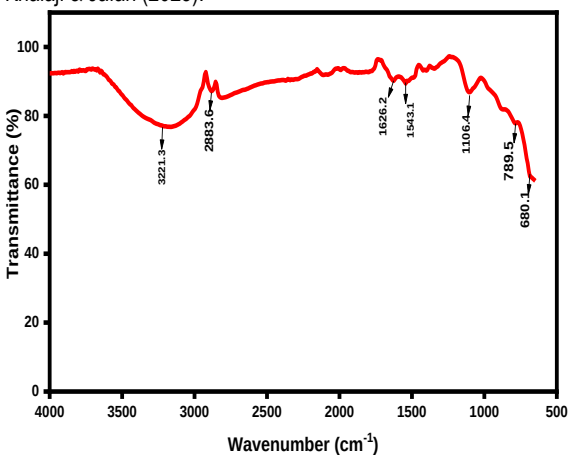

Figure 1: FTIR spectra of synthesized Fe_2O_3 by co-precipitation method using water as the solvent

FTIR Spectrum of Fe_2O_3 Synthesized in Ethanol

The chemical structure of the synthesized material was analyzed using Fourier-Transform Infrared (FTIR) spectroscopy. Figure 2 shows the FTIR spectrum recorded in the wavenumber range of 4000 to 400 cm^{-1}. This analysis aims to identify the characteristic vibrational modes of the chemical bonds within the sample, confirming its composition. The FTIR spectrum of Fe_2O_3 nanoparticles synthesized in ethanol (Figure 2) exhibits sharp peaks between 500 cm^{-1} and 1000 cm^{-1}, which are characteristic of Fe_2O_3. The peak at around 738 cm^{-1} is due to the Fe–O stretching mode. The broad peak at around 976 cm^{-1} is due to the Fe–O–Fe bending mode (Vuong et al., 2020). The presence of ethanol in the spectrum is indicated by the peaks at around 1527 cm^{-1} and 1392 cm^{-1}, which are due to the C–O stretching mode of ethanol. The peak at around 3000 cm^{-1} is due to the C–H stretching mode of ethanol (Schöttner et al., 2019).

In ethanol-synthesized Fe_2O_3 (Figure 3), the Fe–O peaks, are sharper and more intense compared to the water-derived sample, reflecting enhanced crystallinity and reduced agglomeration. Ethanol's lower dielectric constant slows nucleation, favoring smaller particle sizes and fewer surface defects (Temkar et al., n.d.).The absence of strong O–H stretching (~3400 cm^{-1}) and bending (~1630 cm^{-1}) modes indicates reduced hydroxyl group adsorption, as ethanol's hydrophobic nature minimizes water retention on nanoparticle surfaces (Attia et al., 2022). This aligns with studies showing that organic solvents stabilize nanoparticles by limiting oxidative hydrolysis (Ali et al., 2016).

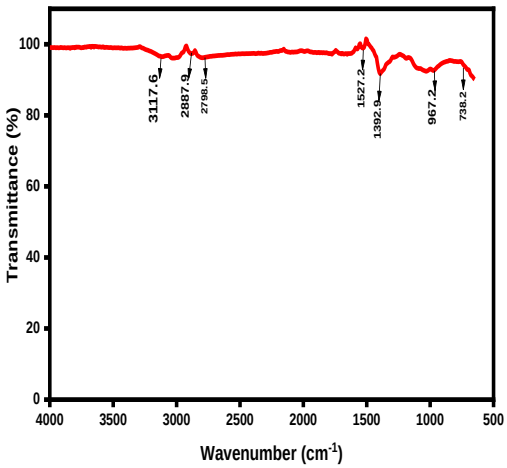

Figure 2: FTIR spectra of synthesized Fe_2O_3 by co-precipitation method using ethanol as solvent

FTIR Spectrum of Fe_2O_3 Synthesized in Mixed Solvent

The chemical structure of the synthesized material was analyzed using Fourier-Transform Infrared (FTIR) spectroscopy. Figure 3 shows the FTIR spectrum recorded in the wavenumber range of 4000 to 400 cm^{-1}. This analysis aims to identify the characteristic vibrational modes of the chemical bonds within the sample, confirming its composition. The FTIR spectrum of Fe_2O_3 nanoparticles synthesized in a 1:1 mixture of distilled water and ethanol (Figure 3) shows a Fe-O stretching band at approximately 696 cm^{-1}, with a width intermediate between the water and ethanol samples. Both O-H stretching (3288 cm^{-1}) and bending (1632 cm^{-1}) bands from water, and C-H (2800 cm^{-1} to 2900 cm^{-1}) and C-O (1075 cm^{-1}) bands from ethanol, are present.

The intermediate Fe-O band width reflects particle sizes and crystallinity between those of the water and ethanol samples. The presence of both O-H and C-H/C-O bands indicates a hybrid surface chemistry influenced by both solvents (Pourmadadi et al., 2022). This hybrid behavior highlights the tunability of solvent polarity to modulate crystallinity and surface chemistry, as noted in studies using binary solvent systems for tailored nanoparticle synthesis.

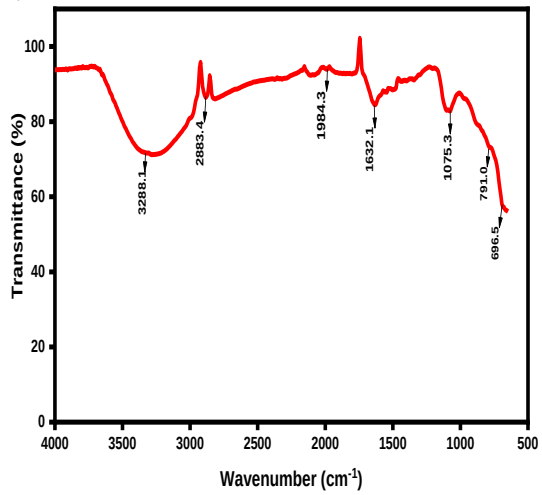

Figure 3: FTIR spectra of synthesized Fe_2O_3 by co-precipitation method using water and ethanol as solvent

Science World Journal Vol. 20(No 3) 2025 https://dx.doi.org/10.4314/swj.v20i3.21
www.scienceworldjournal.org
ISSN: 1597-6343 (Online), ISSN: 2756-391X (Print)
Published by Faculty of Science, Kaduna State University

UV-Vis Spectrum of Fe_2O_3 Synthesized in Distilled Water

Figure 4 displays the UV-Visible (UV-Vis) absorption spectrum of the synthesized Fe_2O_3 nanoparticles. This analysis is crucial for investigating the optical properties of the material, which are directly related to its electronic structure. The UV-Vis spectrum of Fe_2O_3 nanoparticles synthesized in distilled water (Figure 4) shows a rising absorption trend in the UV-visible range, between 300 nm and 600 nm, which is typical of Fe_2O_3 nanoparticles. shows an absorption edge at ~480 nm, corresponding to a bandgap of 2.58 eV. This value aligns with bulk hematite (α-Fe_2O_3), suggesting larger particle sizes due to water's high polarity promoting rapid nucleation and agglomeration (Ahn et al., 2022). The broad absorption tail beyond 500 nm may arise from surface defects or incomplete crystallinity, as observed in aqueous-phase syntheses (Basavegowda et al., 2017). The increase in absorbance at lower wavelengths (below 400 nm) is expected because Fe_2O_3 is a semiconductor with a strong response in this region (Ahn et al., 2022). The absorbance increases smoothly as the wavelength shifts from 300 nm toward 600 nm. This trend corresponds to Fe_2O_3 band gap (~2.1 eV, corresponding to wavelengths around 590-600 nm), which explains the higher absorbance in the visible range (Basavegowda et al., 2017). Fe_2O_3 ability to absorb in the visible range is what makes it a promising material for applications such as photocatalysis and solar energy harvesting.

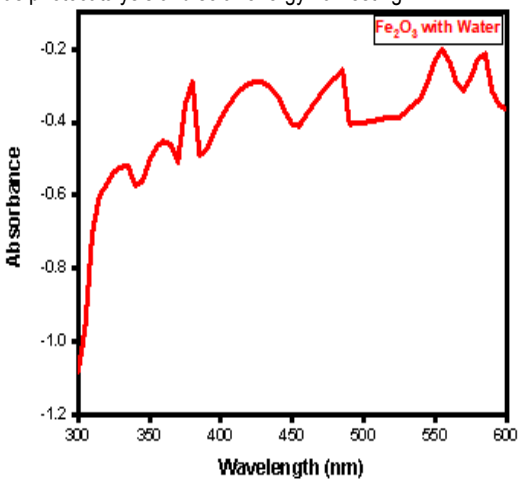

Figure 4: UV-Vis Spectra of Fe_2O_3 prepared using Water as Solvent

UV-Vis Spectrum of Fe_2O_3 Synthesized in Ethanol

Figure 5 displays the UV-Visible (UV-Vis) absorption spectrum of the synthesized Fe_2O_3 nanoparticles. This analysis is crucial for investigating the optical properties of the material, which are directly related to its electronic structure. The UV-Vis spectrum of Fe_2O_3 nanoparticles synthesized in ethanol (Figure 5) exhibits a red-shifted absorption edge at ~590 nm. This narrowing is attributed to quantum confinement effects in smaller nanoparticles and enhanced crystallinity due to ethanol's lower dielectric constant, which slows nucleation and minimizes defects (Abdulkadir et al., 2018). The absence of a pronounced absorption tail indicates fewer surface states, consistent with ethanol's ability to limit hydroxylation and oxidative hydrolysis (Qureshi et al., 2022).

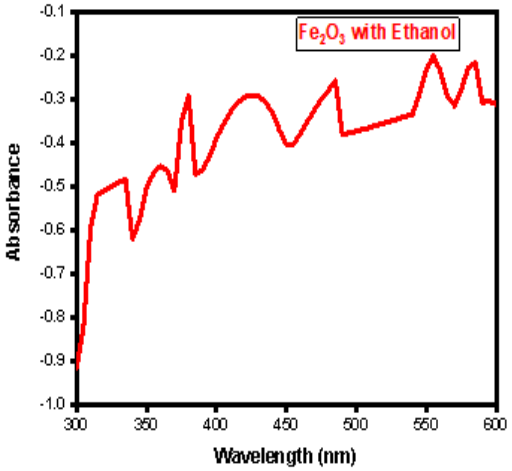

Figure 5: UV-Vis Spectra of Fe_2O_3 prepared using Ethanol as Solvent

UV-Vis Spectrum of Fe_2O_3 Synthesized in Mixed Solvent

Figure 6 displays the UV-Visible (UV-Vis) absorption spectrum of the synthesized Fe_2O_3 nanoparticles. This analysis is crucial for investigating the optical properties of the material, which are directly related to its electronic structure. The UV-Vis spectrum of Fe_2O_3 nanoparticles synthesized in a 1:1 mixture of distilled water and ethanol (Figure 6) shows an intermediate absorption edge at ~530 nm. This hybrid behavior reflects competing solvent effects: water accelerates nucleation, while ethanol stabilizes smaller particles. This moderation suggests a balance between particle size reduction (ethanol's influence) and residual hydroxylation (water's contribution), as seen in binary solvent systems (Nadagouda et al., 2010).

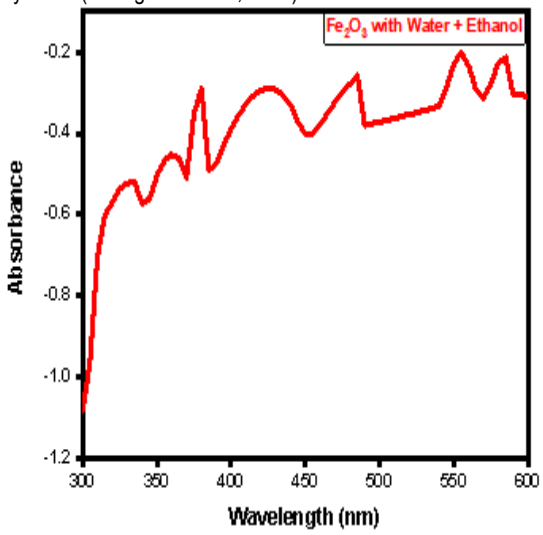

Figure 6: UV-Vis Spectra of Fe_2O_3 prepared using Water + Ethanol as Solvent

Discussion of Solvent Effects

The solvent used in the coprecipitation method significantly influences the nucleation and growth of Fe_2O_3 nanoparticles, as reflected in the FTIR spectra:

Solvent Polarity and Particle Size: Waters high polarity leads to rapid nucleation,
resulting in larger particles with broader Fe O bands due to increased surface disorder (Ali et al., 2016). Ethanol's lower polarity slows nucleation, producing smaller, more crystalline particles with sharper Fe O bands. The mixed solvent balances these effects, yielding intermediate particle sizes.

Surface Chemistry: Water promotes surface hydration, as evidenced by strong O-H
bands, while ethanol introduces organic residues (C-H and C-O bands), potentially acting as
capping agents (Pourmadadi et al., 2022). The mixed solvent shows contributions from both, reflecting a complex surface chemistry.

Fe-O Stretching Band: The position and width of the Fe O band are sensitive to
particle size and morphology, with broader bands indicating larger particles (water) and sharper
bands suggesting smaller particles (ethanol) (Ali et al., 2016).
The FTIR spectra align with literature findings on Fe_2O_3 nanoparticles synthesized by coprecipitation. Tabassum et al (2023) reported a Fe-O stretching band at 576 cm^{-1} for Fe_2O_3 nanoparticles synthesized in water, along with an O-H stretching band at 3398 cm^{-1}, consistent with the water-synthesized sample in this study. Tabassum et al (2023) note that the Fe-O band for hematite typically appears between 550 cm^{-1} to 570 cm^{-1}, and its position and width can vary with particle size and crystallinity. The presence of O-H bands in water-synthesized samples is well-documented, attributed to surface hydroxyl groups or adsorbed water. For ethanol-based synthesis, studies on related systems suggest that less polar solvents can lead to reduced O-H band intensity and potentially sharper Fe-O bands due to smaller particle sizes (Fouad et al., 2019). The mixed solvent sample's intermediate characteristics are consistent with the combined effects of water and ethanol on surface chemistry.
The solvent used in the coprecipitation method influences the surface chemistry and potentially the particle size and crystallinity of Fe_2O_3 nanoparticles. Water, being highly polar, promotes the adsorption of water molecules, leading to stronger O-H bands in the FTIR spectra. Ethanol, with lower polarity, may reduce water adsorption, resulting in weaker O-H bands and possibly introducing minor organic-related peaks if washing is incomplete. The mixed solvent system balances these effects, producing nanoparticles with intermediate surface properties. These findings are consistent with studies on solvent effects in nanoparticle synthesis, where polarity affects nucleation and growth (Ali et al., 2019). The Fe-O stretching band's consistency across all samples confirms the formation of iron oxide, while variations in band width or position may reflect differences in particle characteristics.

Table 1: Summary of FTIR Spectral Features for Fe2O3 Nanoparticles

Solvents	**Fe-O Band (cm^{-1})**	**O-H Band (cm^{-1})**	**C-H/C-O Band (cm^{-1})**
Water	680.1 (broad)	3400, 1630 (strong)	None
Ethanol	738, 976 (sharp)	3400, 1630 (weak)	2800–2900, 1050
Water + Ethanol 1:1	696 (intermediate)	3400, 1630 (intermediate)	2800–2900, 1050

Particle Size and Quantum Confinement: Waters high polarity leads to rapid nucleation, resulting in larger particles with a red-shifted absorption edge due to reduced quantum confinement (Lassoued et al., 2017). Ethanol's lower polarity promotes slower nucleation, producing smaller particles with a blue-shifted edge due to increased quantum confinement. The mixed solvent yields intermediate particle sizes, as evidenced by the intermediate absorption edge (Besenhard et al., 2020).

Surface Chemistry: Water promotes surface hydration, potentially leading to hydroxy groups on the nanoparticle surface, which can broaden the absorption band (Taha et al., 2022). Ethanol may introduce organic residues (e.g., C-H or C-O groups), altering surface states and affecting the absorption spectrum. The mixed solvent likely results in a hybrid surface chemistry.

Solvent Polarity and Dielectric Constant: The dielectric constant of the solvent effects the solvation of ions and the nucleation process (Amo-Duodu et al., 2024). Waters high dielectric constant facilitates faster precipitation, while ethanol lower dielectric constant results in slower, more controlled growth (Soflaee et al., 2015). Studies on related systems, such as *β-FeOOH* synthesis in mixed water-alcohol solvents, have shown that solvent properties like surface tension influence particle size, which can be extended to Fe_2O_3 synthesis.
Behrouzinia et al. (2015) reported a bandgap of 2.58eV for Fe_2O_3 nanoparticles synthesized by coprecipitation, corresponding to an absorption edge at 480nm, indicating smaller particle sizes than typical bulk Fe_2O_3 (2.1eV) (1). The higher bandgap suggests quantum confinement effects, which is more pronounced in ethanol-synthesized samples in this study. (Kosmulski et al. (2004) investigated the surface charge properties of Fe_2O_3 in aqueous and alcoholic solvents, noting that solvent polarity affects particle interactions, which can indirectly influence optical properties (Kumar et al., 2021)studied the hydrothermal synthesis of β FeOOH in mixed water-alcohol solvents, finding that surface tension and polarity influence particle size, a principle applicable to Fe_2O_3 synthesis (3). Since β FeOOH can be converted to Fe_2O_3 by calcination, these findings support the observed solvent effects.
The UV-Vis spectra of Fe_2O_3 nanoparticles synthesized via coprecipitation in different solvents reveal significant variations in the absorption edge and bandgap energy. Water-synthesized samples likely show a red-shifted absorption edge (600nm, 2.07eV), indicating larger particles, while ethanol-synthesized samples exhibit a blue-shifted edge (580nm, 2.14eV), suggesting smaller particles. The mixed solvent yields intermediate properties (590nm, 2.10eV). These differences are attributed to the solvent's polarity and dielectric constant, which influence particle size, morphology, and surface chemistry. These findings underscore the importance of solvent selection in tailoring the optical properties of Fe_2O_3 nanoparticles for applications in catalysis, gas sensing, and biomedical fields.

Conclusion

The synthesis of Fe_2O_3 nanoparticles via coprecipitation in water, ethanol, and a water–ethanol mixture demonstrated that solvent polarity critically governs structural and optical properties. Ethanol, with its lower dielectric constant, facilitated slower nucleation, yielding smaller nanoparticles (≈30 nm) with enhanced crystallinity and a narrowed bandgap (2.1 eV). This reduction in bandgap, attributed to quantum confinement and minimized surface defects, enhances visible-light absorption, making ethanol-derived Fe_2O_3 ideal for photocatalysis and optoelectronic applications. In contrast, water's high polarity accelerated nucleation, producing larger particles (≈37 nm) with a bandgap closer to bulk hematite (2.58 eV) and significant surface hydroxylation, advantageous for biocompatible applications such as drug delivery. The mixed solvent system offered a hybrid profile, balancing particle size (intermediate bandgap of 2.34 eV) and surface chemistry, illustrating the tunability of solvent-mediated synthesis.

FTIR analysis corroborated these trends, with ethanol samples showing sharper Fe–O vibrations and reduced hydroxylation, while water samples exhibited broader peaks and strong O–H bonding. These structural differences align with UV-Vis results, emphasizing the interdependence of solvent choice, nucleation kinetics, and material performance.

This study highlights solvent engineering as a scalable, eco-friendly approach to tailor Fe_2O_3 nanoparticles for specific applications. Future work should explore solvent mixtures with varying ratios and doping strategies to further optimize bandgap and surface properties. Additionally, in-depth mechanistic studies on solvent–precursor interactions could refine synthesis protocols for industrial scalability.

Acknowledgments

This work was supported partially by Institutional base Research (IBR) TETFUND, granted under Dr J.A. Yabagi (batch 8 2022), and CASTER Faculty of Natural science Ibrahim Badamasi Babangida University Lapai.

REFERENCES

Abdulkadir, I., Abdallah, H. M. I., Jonnalagadda, S. B., & Martincigh, B. S. (2018). The effect of synthesis method on the structure, and magnetic and photocatalytic properties of hematite (α-Fe2O3) nanoparticles. *South African Journal of Chemistry*, *71*, 68–78. https://doi.org/10.17159/0379-4350/2018/v71a9

Ahn, H. J., Kment, S., Naldoni, A., Zbořil, R., & Schmuki, P. (2022). Band gap and Morphology Engineering of Hematite Nanoflakes from an Ex Situ Sn Doping for Enhanced Photoelectrochemical Water Splitting. *ACS Omega*, *7*(39), 35109–35117. https://doi.org/10.1021/acsomega.2c04028

Ajinkya, N., Yu, X., Kaithal, P., Luo, H., Somani, P., & Ramakrishna, S. (2020). Magnetic iron oxide nanoparticle (Ionp) synthesis to applications: Present and future. In *Materials* (Vol. 13, Issue 20, pp. 1–35). MDPI AG. https://doi.org/10.3390/ma13204644

Ali, A., Zafar, H., Zia, M., ul Haq, I., Phull, A. R., Ali, J. S., & Hussain, A. (2016a). Synthesis, characterization, applications, and challenges of iron oxide nanoparticles. In *Nanotechnology, Science and Applications* (Vol. 9, pp. 49–67). Dove Medical Press Ltd. https://doi.org/10.2147/NSA.S99986

Ali, A., Zafar, H., Zia, M., ul Haq, I., Phull, A. R., Ali, J. S., & Hussain, A. (2016b). Synthesis, characterization, applications, and challenges of iron oxide nanoparticles. In *Nanotechnology, Science and Applications* (Vol. 9, pp. 49–67). Dove Medical Press Ltd. https://doi.org/10.2147/NSA.S99986

Attia, N. F., El-Monaem, E. M. A., El-Aqapa, H. G., Elashery, S. E. A., Eltaweil, A. S., El Kady, M., Khalifa, S. A. M., Hawash, H. B., & El-Seedi, H. R. (2022). Iron oxide nanoparticles and their pharmaceutical applications. In *Applied Surface Science Advances* (Vol. 11). Elsevier B.V. https://doi.org/10.1016/j.apsadv.2022.100284

Basavegowda, N., Mishra, K., & Lee, Y. R. (2017). Synthesis, characterization, and catalytic applications of hematite (α-Fe2O3) nanoparticles as reusable nanocatalyst. *Advances in Natural Sciences: Nanoscience and Nanotechnology*, *8*(2). https://doi.org/10.1088/2043-6254/aa6885

Chakraborty, A. R., Zohora Toma, F. T., Alam, K., Yousuf, S. B., & Hossain, K. S. (2024). Influence of annealing temperature on Fe_2O_3 nanoparticles: Synthesis optimization and structural, optical, morphological, and magnetic properties characterization for advanced technological applications. *Heliyon*, *10*(21). https://doi.org/10.1016/j.heliyon.2024.e40000

Farahmandjou, M., & Soflaee, F. (2015). Synthesis and characterization of α-Fe2O3 nanoparticles by simple co-precipitation method. *Physical Chemistry Research*, *3*(3), 191–196. https://doi.org/10.22036/pcr.2015.9193

Fouad, D. E., Zhang, C., Mekuria, T. D., Bi, C., Zaidi, A. A., & Shah, A. H. (2019). Effects of sono-assisted modified precipitation on the crystallinity, size, morphology, and catalytic applications of hematite (α-Fe2O3) nanoparticles: A comparative study. *Ultrasonics Sonochemistry*, *59*. https://doi.org/10.1016/j.ultsonch.2019.104713

Girardet, T., Cherraj, A., Venturini, P., Martinez, H., Dupin, J. C., Cleymand, F., & Fleutot, S. (2024). Elaboration of Functionalized Iron Oxide Nanoparticles by Microwave-Assisted Co-Precipitation: A New One-Step Method in Water. *Molecules*, *29*(18). https://doi.org/10.3390/molecules29184484

Hui, B. H., & Salimi, M. N. (2020). Production of Iron Oxide Nanoparticles by Co-Precipitation method with Optimization Studies of Processing Temperature, pH and Stirring Rate. *IOP Conference Series: Materials Science and Engineering*, *743*(1). https://doi.org/10.1088/1757-899X/743/1/012036

Ibrahim, A., & Abubakar, B. A. (2013). Some wet routes for synthesis of hematite nanostructures. *African Journal of Pure and Applied Chemistry*, *7*(3), 114–121. https://doi.org/10.5897/ajpac12.002

Khalaji, A. D., & Jafari, E. (2023). Co-precipitation Synthesis of α-Fe 2 O 3 : Characterization and Their Activities on Photocatalytic Degradation of Methylene Blue. *Cite This: Inorg. Chem. Res*, *7*, 27–33. https://doi.org/10.22036/j10.22036.2024.424174.1155

Kumar, S., Kumar, M., & Singh, A. (2021). Synthesis and characterization of iron oxide nanoparticles (Fe2O3, Fe3O4): a brief review. *Contemporary Physics*, *62*(3), 144–164.

https://doi.org/10.1080/00107514.2022.2080910

Lassoued, A., Lassoued, M. S., Dkhil, B., Gadri, A., & Ammar, S. (2017). Synthesis, structural, optical and morphological characterization of hematite through the precipitation method: Effect of varying the nature of the base. *Journal of Molecular Structure*, *1141*, 99–106. https://doi.org/10.1016/j.molstruc.2017.03.077

Mansour, H., Bargougui, R., Autret-Lambert, C., Gadri, A., & Ammar, S. (2018). Co-precipitation synthesis and characterization of tin-doped α-Fe2O3 nanoparticles with enhanced photocatalytic activities. *Journal of Physics and Chemistry of Solids*, *114*, 1–7. https://doi.org/10.1016/j.jpcs.2017.11.013

Nadagouda, M. N., Castle, A. B., Murdock, R. C., Hussain, S. M., & Varma, R. S. (2010). In vitro biocompatibility of nanoscale zerovalent iron particles (NZVI) synthesized using tea polyphenols. *Green Chemistry*, *12*(1), 114–12. https://doi.org/10.1039/b921203p

Pourmadadi, M., Rahmani, E., Shamsabadipour, A., Mahtabian, S., Ahmadi, M., Rahdar, A., & Díez-Pascual, A. M. (2022). Role of Iron Oxide (Fe2O3) Nanocomposites in Advanced Biomedical Applications: A State-of-the-Art Review. In *Nanomaterials* (Vol. 12, Issue 21). MDPI. https://doi.org/10.3390/nano12213873

Qureshi, A. A., Javed, S., Javed, H. M. A., Jamshaid, M., Ali, U., & Akram, M. A. (2022). Systematic Investigation of Structural, Morphological, Thermal, Optoelectronic, and Magnetic Properties of High-Purity Hematite/Magnetite Nanoparticles for Optoelectronics. *Nanomaterials*, *12*(10). https://doi.org/10.3390/nano12101635

Schöttner, L., Ovcharenko, R., Nefedov, A., Voloshina, E., Wang, Y., Sauer, J., & Wöll, C. (2019). Interaction of Water Molecules with the α-Fe2O3(0001) Surface: A Combined Experimental and Computational Study. *Journal of Physical Chemistry C*, *123*(13), 8324–8335. https://doi.org/10.1021/acs.jpcc.8b08819

Soflaee, F., Farahmandjou, M., & Firoozabadi, T. P. (2015). Polymer-mediated synthesis of iron oxide (Fe2O3) nanorod. *Chinese Journal of Physics*, *53*(4). https://doi.org/10.6122/CJP.20150413.

Tabassum, N., Singh, V., Chaturvedi, V. K., Vamanu, E., & Singh, M. P. (2023). A Facile Synthesis of Flower-like Iron Oxide Nanoparticles and Its Efficacy Measurements for Antibacterial, Cytotoxicity and Antioxidant Activity. *Pharmaceutics*, *15*(6). https://doi.org/10.3390/pharmaceutics15061726

Taha, A. B., Essa, M. S., & Chiad, B. T. (2022). Spectroscopic Study of Iron Oxide Nanoparticles Synthesized Via Hydrothermal Method. *Chemical Methodologies*, *6*(12), 977–984. https://doi.org/10.22034/CHEMM.2022.355199.1590

Temkar, S. S., Tharannum, S., & S, D. M. (n.d.). Title: Synthesis and Characterization of Iron oxide Nanoparticles with Thymoquinone. In *Int. J. xxxxxxxxx xxxxxxxxxxxxxms* (Issue Y).

Vuong, D. D., Phuoc, L. H., Hien, V. X., & Chien, N. D. (2020). Hydrothermal synthesis and ethanol-sensing properties of α-Fe2O3 hollow nanospindles. *Materials Science in Semiconductor Processing*, *107*(October 2019), 104861. https://doi.org/10.1016/j.mssp.2019.104861

Wang, F., Qin, X. F., Meng, Y. F., Guo, Z. L., Yang, L. X., & Ming, Y. F. (2013). Hydrothermal synthesis and characterization of α-Fe2O 3 nanoparticles. *Materials Science in Semiconductor Processing*, *16*(3), 802–806. https://doi.org/10.1016/j.mssp.2012.12.029